INDIAN JOURNAL OF SCIENCE AND TECHNOLOGY

RESEARCH ARTICLE

OPEN ACCESS

Received: 28.03.2021

Accepted: 02.08.2021

Published: 18.08.2021

Citation: Ch Komali , Murali N, Parajuli D, Ramakrishna A, Ramakrishna Y, Chandramouli K (2021) Effect of Cu^{2+} substitution on structure, morphology, and magnetic properties of Mg-Zn spinel ferrite. Indian Journal of Science and Technology 14(27): 2309-2316. https://doi.org/10.17485/IJST/v14i27.527

* **Corresponding author**.

muraliphdau@gmail.com

Funding: None

Competing Interests: None

Published By Indian Society for Education and Environment (iSee)

ISSN
Print: 0974-6846
Electronic: 0974-5645

Effect of Cu^{2+} substitution on structure, morphology, and magnetic properties of Mg-Zn spinel ferrite

Ch Komali[1], N Murali[1]*, D Parajuli[2], A Ramakrishna[3], Y Ramakrishna[1], K Chandramouli[1]

1 Department of Engineering Physics, AUCE (A), Andhra University, Visakhapatnam
2 Department of Physics, AUCST, Andhra University, Visakhapatnam
3 Department of ECE, Aditya College of Engineering and Technology, Surampalem, Kakinada, India

Abstract

Objective: To prepare Cu doped $Mg_{0.5-x}Cu_xZn_{0.5}Fe_2O_4$ (x = 0.0, 0.05, 0.1, 0.15, 0.2 and 0.25) spinel ferrites materials and study the structure, morphology, and magnetic properties. **Methods:** Cu doped Mg-Zn spinel ferrites are magnetic and highly resistive materials. They were synthesized by the method of solid-state reaction and characterized by x-ray diffraction (XRD), field effect scanning electron microscopy (FESEM), Fourier transform infrared (FTIR), and vibrating sample magnetometer (VSM) for their structural, compositional, morphological, functional properties. They are with spinel structure under Fd-3m space group. Their crystallite size was 44.58 nm to 31.02 nm range after calcined at 1000 ^oC. Their spinel structure was confirmed with FT-IR analysis, whose absorption bands were 598.84 – 580.40 cm^{-1} and 405.35 - 402.15 cm^{-1} range for higher and lower frequency, respectively. The value of coercivity is in the range 146.33 - 9.427 Oe with the variation of content. The lower values of the coercivity indicated the soft ferrimagnetic nature of the synthesized materials. **Findings/ Application:** Substitution of non-magnetic Cu^{2+} ions strongly influenced the structural and magnetic properties of magnesium ferrites.

Keywords: Cu doped MgZn ferrite; XRD; FTIR; FESEM; Coercivity

1 Introduction

In the spinel ferrites family, magnesium ferrite ($MgFe_2O_4$) has a spinel structure with inversion mode that depends on the synthesis method used in memory and switching circuits. Magnesium ferrite is used in heterogeneous catalysis, adsorption, sensors, and magnetic technologies[1–4]. The non-magnetic Cu resides in a tetrahedral (A) site whose doping can modify the structural, electrical, and magnetic properties[5–7]. Doping of Al[8,9], Ge[10], Cu[11], Ni[12], Cr[13], Sm-Gd[14], Ce-Gd[15] on magnesium ferrite and their effects on the electrical, dielectric and magnetic properties were studied[16–18]. However, solid-state synthesis was rarely used, which has a different impact on the sample size[19].

In the present study, the spinel ferrite with the generic formula Cu doped $Mg_{0.5-x}Cu_xZn_{0.5}Fe_2O_4$ (x = 0.0, 0.05, 0.1, 0.15, 0.2, and 0.25) was prepared by the standard ceramic method. The structural and magnetic properties were investigated using x-ray diffraction, field effect scanning electron microscopy, infrared spectroscopy, and vibrating sample magnetometer.

2 Materials and Methods

MgO, ZnO, CuO, and Fe_2O_3 were mixed in appropriate stoichiometric ratio, finely grounded for 3-4 h, pre-sintered at 800 °C for 5 h, again reground for 3-4 h and finally calcined at 1000 °C for 6 h and prepared Cu doped $Mg_{0.5-x}Cu_xZn_{0.5}Fe_2O_4$ (x = 0.0, 0.05, 0.1, 0.15, 0.2 and 0.25) under solid-state reaction method. The discs-shaped pallet was prepared from the resultant powder with the hydraulic press's help under 6 ton/cm^2 pressure and finally sintered at 1200 °C for 4 h, and measured the magnetic properties. Every heating process was followed by cooling.

The structural data were studied XRD (PANalytical XPert PRO diffractometer with CuKα radiation and λ = 1.5402 Å also with a continuous scan step size of 0.008). The morphology data were studied Scanning Electron Microscope (Carl Zeiss, EVOMA 15, Oxford Instruments, Inca Penta FETx3.JPG instrument). The chemical bonding data were examined FTIR (IR Prestige21 Shimadzu). Finally, magnetic properties were studied VSM (1T).

3 Results and Discussion

3.1 X-ray diffraction studies

The structure of Cu doped $Mg_{0.5-x}Cu_xZn_{0.5}Fe_2O_4$ (x = 0.0, 0.05, 0.1, 0.15, 0.2 and 0.25) ferrite samples were characterized by x-ray diffraction technique in the 2θ range of 20-80 degree with Cu-Kα radiation of wavelength λ = 1.5406 Å at room temperature shown in Figure 1. Bragg's law was used for indexing the XRD patterns related to planes (220), (311), (400), (422), (511), and (440), it's found the single-phase cubic spinel structure of all the samples[20]. The crystallite size and lattice parameter are listed in Table 1. Thus, the synthesized materials are in the nanoscale range, exhibiting the nanoparticle behaviors applicable in different technological outputs. The highest lattice parameter with the least crystallite size and such parameters impact not only the structure but also the magnetic and electrical properties.

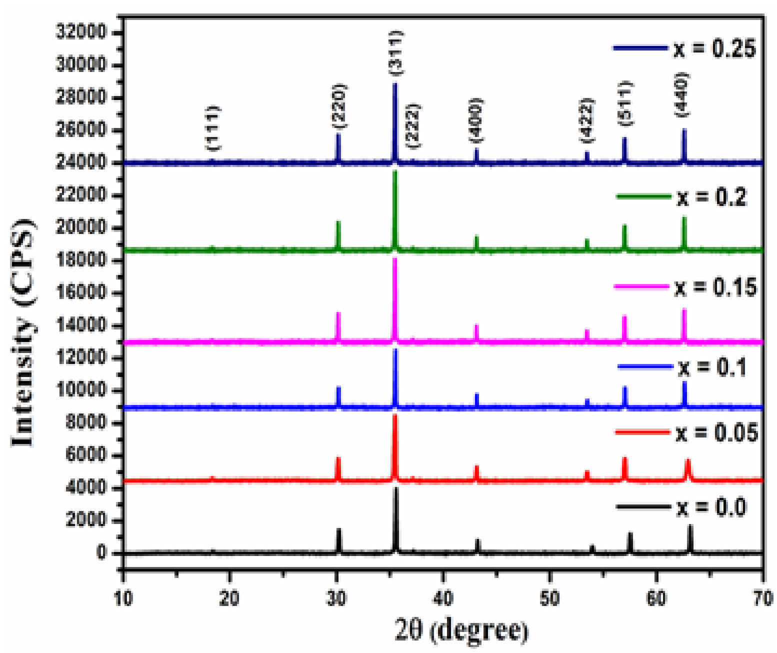

Fig 1. XRD patterns of Cu doped Mg-Zn-Cu ferrites

Table 1. Lattice constant (a) and Crystallite size (D) of Cu doped Mg-Zn ferrite

Compounds	Lattice constant a (Å)	Crystallite size (nm)
0.0	8.413	44.58
0.05	8.417	42.12
0.1	8.419	39.54
0.15	8.421	36.49
0.2	8.424	33.85
0.25	8.429	31.02

The lattice constants (a) of the samples were calculated using standard relation [21],

$$\frac{1}{d^2} = \frac{h^2 + k^2 + l^2}{a^2}$$

where (d) is inter-planar spacing; (h k l) is Miller Indices.

The lattice constant is increasing gradually with Cu content due to the larger ionic radius of the Cu^{2+} (0.70 Å) than that of the Mg^{2+} (0.65 Å) as shown in Figure 2 and agrees with previous literature [22]. The crystallite size of the synthesized Cu doped Mg-Zn ferrite powders was evaluated with the help of Debye- Scherrer's relation [23],

$$D = \frac{K\lambda}{\beta \cos\theta}$$

where λ, β, and θ are the radiation's wavelength, the full width half maximum (FWHM) of the XRD peak, and Bragg's angle.

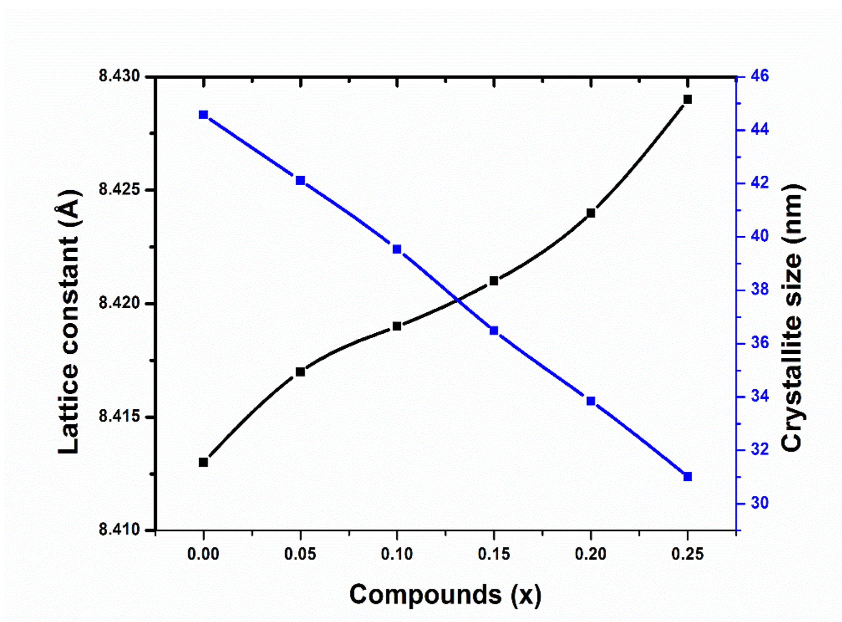

Fig 2. Variation of lattice constant and crystallite size of Cu-dopedMgZn ferrites

3.2 FESEM studies

The room temperature morphological study of the present Cu doped $Mg_{0.5-x}Cu_xZn_{0.5}Fe_2O_4$ (x = 0.0, 0.5, 0.1, 0.15, 0.2 and 0.25) synthesized materials was carried out using a scanning electron microscopy. The obtained FESEM micrographs are presented in Figure 3. Using these images, grain size for all the samples was obtained. Further, a more significant part of pores is on the scale of grain size and located among them [24]. Some aggregates are also observed in the micrographs. From micrographs exhibited cubic crystals of uniform size with average values between 2.7 to 4.6 Ωm.

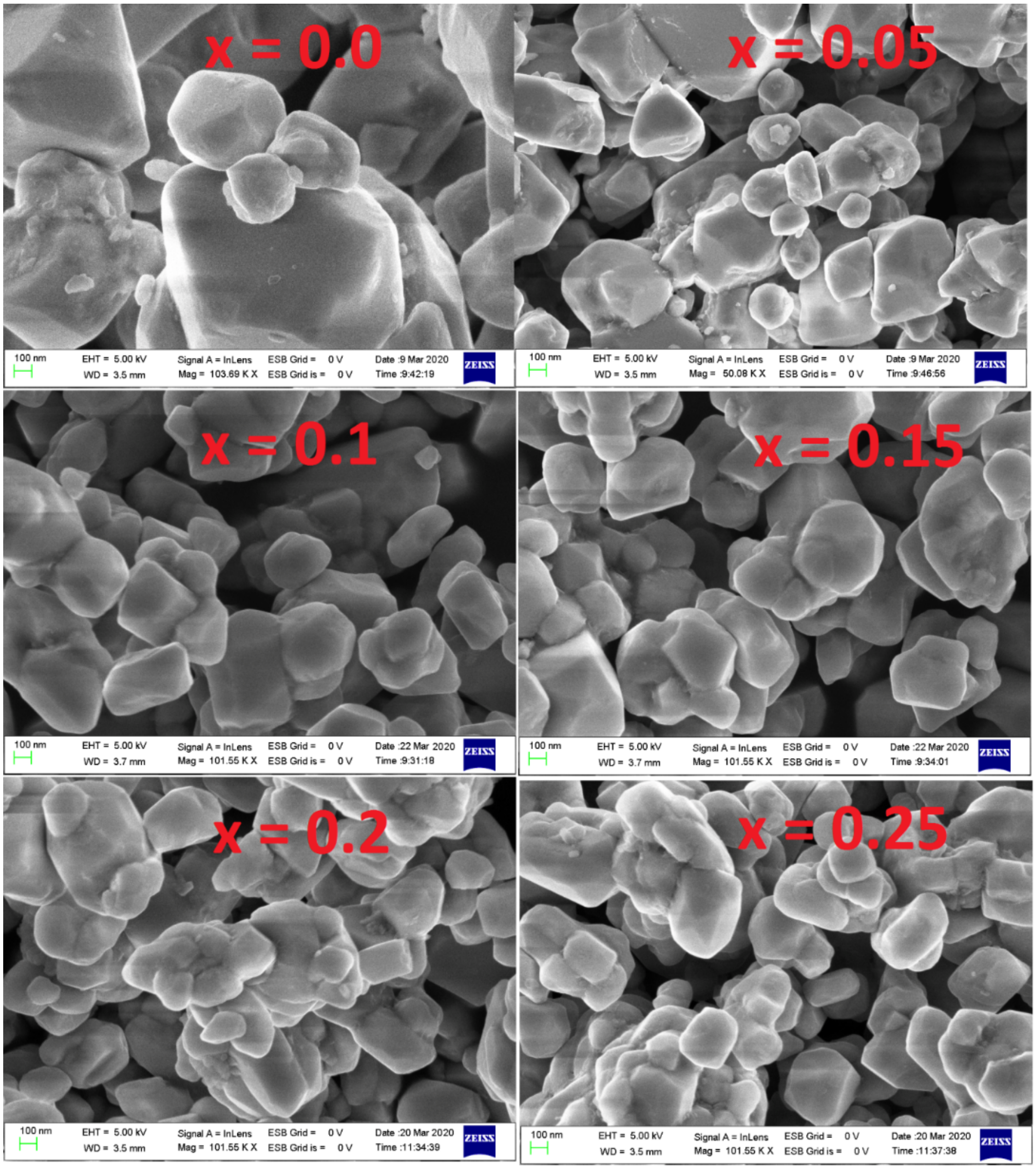

Fig 3. FESEM images of Cu doped Mg-Zn ferrite samples

3.3 FTIR studies

The infrared spectra of all the Cu doped $Mg_{0.5-x}Cu_xZn_{0.5}Fe_2O_4$ (x = 0.0, 0.05, 0.1, 0.15, 0.2 and 0.25) are presented in Figure 4. They all have two prominent absorption bands ν_1 and $\nu_{2,}$ in 600 and 400 cm^{-1}, due to stretching of tetrahedral metal ion-oxygen bonding and vibrations of oxygen perpendicular to the axis joining the tetrahedral ion-oxygen respectively, as listed in Table 2. In the present system, the band ν_1 is found in the range of 598.84–580.40 cm^{-1}, and the lower band is in the range of 405.35-402.15 cm^{-1}. The band positions obtained in the present case are found to be in the reported range[25]. Slight variation in the band positions is due to the present samples' preparation, grain size, and porosity. Further, the absorption bands ν_1 assigned to the tetrahedral site (A) are shifted towards the lower frequency side with an increase in the Cu substitution. The band positions' variation can be attributed to the estimated cation distribution of the present ferrite samples [26].

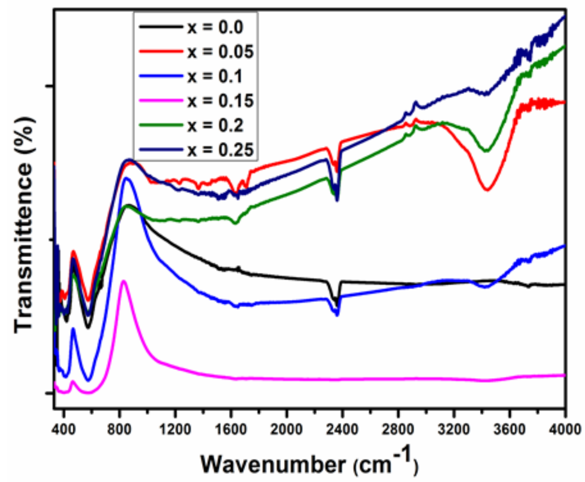

Fig 4. Infrared spectra Cu doped Mg-Zn ferrites

Table 2. Absorption bands of Cu doped Mg-Znferrites

Concentration (**x**)	Tetrahedral υ_1 (**cm^{-1}**)	Octahedral υ_2 (**cm^{-1}**)
0.0	580.40	402.15
0.05	582.85	403.48
0.1	585.92	404.46
0.15	591.05	407.85
0.2	598.84	405.35

3.4 Magnetic properties study

The ceramically prepared Cu doped $Mg_{0.5-x}Cu_xZn_{0.5}Fe_2O_4$ (x = 0.0, 0.05, 0.1, 0.15, 0.2 and 0.25) ferrite particles' magnetic properties were studied using vibrating sample magnetometer (VSM) [27]. All the measurements of the magnetic properties were carried out at room temperature. The hysteresis loops are shown in Figure 5.

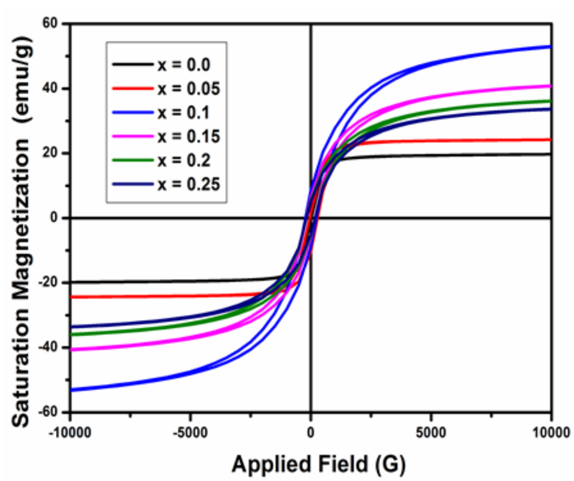

Fig 5. Hysteresis loops Cu doped Mg-Zn ferrites

The saturation magnetization (M_s) and coercivity (H_c) were obtained from the hysteresis loops, and the obtained values as listed in Table 3 and variation are shown in Figure 6. The table shows that the saturation magnetization increases with an increase in Cu substitution x = 0.1 and decreases x = 0.25. The highest saturation magnetization for magnesium ferrite is found to be 53.51 emu/g (x = 0.1). The coercivity is found to reduce from 146.33 Oe to 9.427Oe with the substitution of Cu. This implies that Neel's model could explain the observed magnetic behaviour of the Cu doped Mg-Zn samples.

Table 3. Ms and Hc values of Cu doped Mg-Zn ferrites

Concentration	M_s **(emu/g)**	H_c **(Oe)**
0.0	19.66	146.33
0.05	24.26	112.05
0.1	53.51	69.56
0.15	40.86	43.25
0.2	36.02	29.48
0.25	33.81	9.427

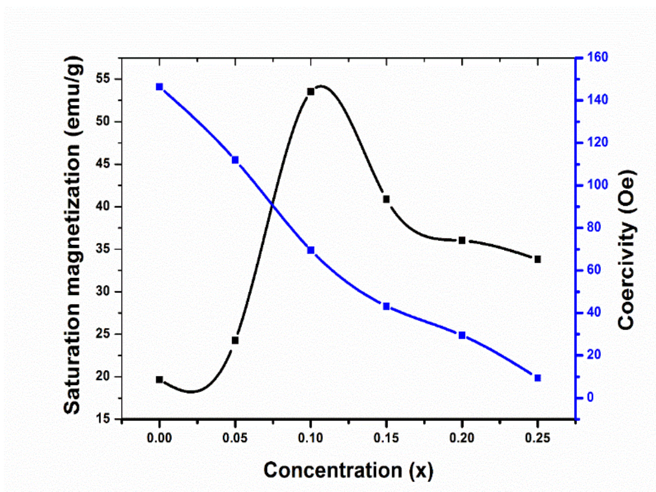

Fig 6. Variation of saturation magnetization andcoercivity of Cu doped Mg-Zn ferrites

Neel's theory of ferrimagnetism suggests that the cations present on various sublattices in spinel structure have attractive minutes oppositely adjusted. The inverse spinel ferrites of the net magnetic moment mainly depend on the number of magnetic ions that occupy the tetrahedral and octahedral sites[28]. The Cu^{2+} ions substituted in synthesized samples have a direct bearing on the coercivity. Ongoing investigations proposed that coercivity was influenced by microstrain, size dissemination, magneto crystallinity, attractive area size, and anisotropy[29,30].

4 Conclusions

Cu doped $Mg_{0.5-x}Cu_xZn_{0.5}Fe_2O_4$ (x = 0.0, 0.05, 0.1, 0.15, 0.2 and 0.25) ferrite are prepared by solid-state reaction method. The samples were of single-phase, cubic spinel structure according to XRD. The gradual increase in lattice constant values with Cu substitution is obviously due to the Cu's larger ionic radius than the Mg. SEM micrographs exhibited cubic crystals of uniform size with average values between 2.7 to 4.6 Ωm. Infrared spectroscopic studies supported the spinel structure of all the ferrites. VSM studies revealed that the saturation magnetization is increased with increased Cu substitution from their highest values, 53.51 emu/g to 19.66 emu/g, respectively. On the other hand, the coercivity decreases from 146.33 Oe to 9.427 Oe with an increase in substitution. Thus, the substitution of non-magnetic Cu ions in magnesium has strongly influenced the magnesium ferrite's structural and magnetic properties.

References

1) Ortiz-Quiñonez JL, Pal U, Villanueva MS. Structural, magnetic, and catalytic evaluation of spinel Co, Ni, and Co-Ni ferrite nanoparticles fabricated by low-temperature solution combustion process. *ACS omega*. 2018;3:14986–15001. Available from: https://pubs.acs.org/doi/abs/10.1021/acsomega.8b02229.
2) Himakar P, Murali N, Parajuli D, Veeraiah V, Samatha K, Mammo TW, et al. Magnetic and DC Electrical Properties of Cu Doped Co-Zn Nanoferrites. *Journal of Electronic Materials*;2021:1–9. Available from: https://link.springer.com/article/10.1007/s11664-021-08760-8.
3) Ramakrishna A, Murali N, Mammo TW, Samatha K, Veeraiah V. Structural and DC electrical resistivity, magnetic properties of Co0.5M0.5Fe2O4 (M= Ni, Zn, and Mg) ferrite nanoparticles. *Physica B: Condensed Matter*. 2018;534:134–140. Available from: https://doi.org/10.1016/j.physb.2018.01.033.
4) Sagar TV, Rao TS, Naidu KC. AC-electrical conductivity, magnetic susceptibility, dielectric modulus and impedance studies of sol-gel processed nano-NiMgZn ferrites. *Materials Chemistry and Physics*. 2021;258(123902). Available from: https://doi.org/10.1016/j.matchemphys.2020.123902.
5) Kambale RC, Shaikh PA, Bhosale CH, Rajpure KY, Kolekar YD. The effect of Mn substitution on the magnetic and dielectric properties of cobalt ferrite synthesized by an autocombustion route. *Smart Materials and structures*. 2009;18. Available from: https://iopscience.iop.org/article/10.1088/0964-1726/18/11/115028/meta.
6) Mehaka, Somnath, Sharma I, Batoo KM, Kumar G. Cation distribution and structural study of copper doped magnesium-manganese nanoferrites. *Materials Today: Proceedings 2020*;26:3473–3477. Available from: https://doi.org/10.1016/j.matpr.2020.01.203.
7) Raju G, Murali N, Prasad MSNA, Suresh B, Babu DA, Kiran MG, et al. Effect of chromium substitution on the structural and magnetic properties of cobalt ferrite. *Materials Science for Energy Technologies*. 2019;2(1):78–82. Available from: https://doi.org/10.1016/j.mset.2018.11.001.
8) Mercy SJ, Murali N, Ramakrishna A, Ramakrishna Y, Veeraiah V, Samatha K. Microstructural, thermal, electrical and magnetic analysis of Mg2+ substituted Cobalt ferrite. *Applied Physics A*. 2020;2020(126):1–13. Available from: https://doi.org/10.1007/s00339-020-04048-6.
9) Ansari F, Sobhani A, Salavati-Niasari M. Simple sol-gel synthesis and characterization of new CoTiO3/CoFe2O4 nanocomposite by using liquid glucose, maltose and starch as fuel, capping and reducing agents. *Journal of colloid and interface science*;2018(15):723–732. Available from: https://doi.org/10.1016/j.jcis.2017.12.083.
10) Desai SS, Shirsath SE, Batoo KM, Adil SF, Khan M, Patange SM. Influence of Zn-Zr substitution on the crystal chemistry and magnetic properties of CoFe2O4 nanoparticles synthesized by sol-gel method. *Physica B: Condensed Matter*. 2020;596(412400). Available from: https://doi.org/10.1016/j.physb.2020.412400.
11) Ramakrishna A, Murali N, Margarette SJ, Samatha K, Veeraiah V. Comparative study of synthesis, structural and magnetic properties of Cu2+ substituted Co-Ni, Co-Zn and Co-Mg nano ferrites. *Physica B: Condensed Matter*. 2018;530:251–257. Available from: https://doi.org/10.1016/j.physb.2017.11.063.
12) Nlebedim IC, Jiles DC. Suitability of cation substituted cobalt ferrite materials for magnetoelastic sensor applications. *Smart Materials and Structures*. 2014;24(25006). Available from: https://iopscience.iop.org/article/10.1088/0964-1726/24/2/025006/meta.
13) Rao PA, Raghavendra V, Suryanarayana B, Paulos T, Murali N, Varma PP, et al. Cadmium substitution effect on structural, electrical and magnetic properties of Ni-Zn nano ferrites. *Results in Physics*. 2020;19(103487). Available from: https://doi.org/10.1016/j.rinp.2020.103487.
14) Dippong T, Levei EA, Deac IG, Neag E, Cadar O. Influence of Cu2+, Ni2+, and Zn2+ ions doping on the structure, morphology, and magnetic properties of co-ferrite embedded in sio2 matrix obtained by an innovative sol-gel route. *Nanomaterials*. 2020;10(3). Available from: https://doi.org/10.3390/nano10030580.
15) Mammo TW, Murali N, Sileshi YM, Arunamani T. Effect of Ce-substitution on structural, morphological, magnetic and DC electrical resistivity of Co-ferrite materials. *Physica B: Condensed Matter*. 2018;531(15):164–170. Available from: https://doi.org/10.1016/j.physb.2017.12.049.
16) Dabagh S, Ati AA, Ghoshal SK, Zare S, Rosnan RM, Jbara AS, et al. Cu2+ and Al3+ co-substituted cobalt ferrite: structural analysis, morphology and magnetic properties. *Bulletin of Materials Science*. 2016;39:1029–1037. Available from: https://link.springer.com/article/10.1007/s12034-016-1233-8.
17) Mammo TW, Kumari CV, Margarette SJ, Ramakrishna A, Vemuri R, Rao YS, et al. Synthesis, structural, dielectric and magnetic properties of cobalt ferrite nanomaterial prepared by sol-gel autocombustion technique. *Physica B: Condensed Matter*. 2020;581(15). Available from: https://doi.org/10.1016/j.physb.2019.411769.
18) Maria KH, Choudhury S, Hakim MA. Structural phase transformation and hysteresis behavior of Cu-Zn ferrites. *International Nano Letters*. 2013;3:1–10. Available from: https://link.springer.com/article/10.1186/2228-5326-3-42.
19) Tedjieukeng HMK, Tsobnang PK, Fomekong RL, Etape EP, Joy PA, Delcorte A, et al. Structural characterization and magnetic properties of undoped and copper-doped cobalt ferrite nanoparticles prepared by the octanoate coprecipitation route at very low dopant concentrations. *RSC advances* . 2018;8:38621–38630. Available from: https://doi.org/10.1039/C8RA08532C.
20) Torkian S, Ghasemi A, Razavi S, Tavoosi RM. Structural and Magnetic Properties of High Coercive Al-Substituted Strontium Hexaferrite Nanoparticles. *Journal Superconductivity and Novel Magnetism*. 2016;29:1627–1640. Available from: https://link.springer.com/article/10.1007/s10948-016-3450-1.
21) Desai SS, Shirsath SE, Batoo KM, Adil SF, Khan M, Patange SM. Influence of Zn-Zr substitution on the crystal chemistry and magnetic properties of CoFe2O4 nanoparticles synthesized by sol-gel method. *Physica B: Condensed Matter*. 2020;596(1). Available from: https://doi.org/10.1016/j.physb.2020.412400.
22) Dar MA, Shah J, Siddiqui WA, Kotnala RK. Study of structure and magnetic properties of Ni-Zn ferrite nano-particles synthesized via co-precipitation and reverse micro-emulsion technique. *Applied Nanoscience*. 2014;4:675–682. Available from: https://link.springer.com/article/10.1007/s13204-013-0241-x.
23) Raghasudha M, Ravinder D, Veerasomaiah P. Effect of Cr Substitution on magnetic properties of Mg nanoferrites synthesized by citrate-gel auto combustion method. *Journal of Chemistry*. 2013;2013. Available from: https://www.hindawi.com/journals/jchem/2013/804042/.
24) Routray KL, Saha S, Sanyal D, Behera D. Role of rare-earth (Nd3+) ions on structural, dielectric, magnetic and Mossbauer properties of nano-sized CoFe2O4: useful for high frequency application. *Materials Research Express*. 2018;6. Available from: https://iopscience.iop.org/article/10.1088/2053-1591/aaf2b5/meta.
25) Kurian M, Thankachan S, Nair DS, Aswathy EK, Babu A, Thomas A, et al. Structural, magnetic, and acidic properties of cobalt ferrite nanoparticles synthesised by wet chemical methods. *Journal of Advanced Ceramics*. 2015;4:199–205. Available from: https://link.springer.com/article/10.1007/s40145-015-0149-x.
26) Qamar S, Akhtar MN, Batoo KM, Raslan EH. Structural and magnetic features of Ce doped Co-Cu-Zn spinel nanoferrites prepared using sol gel self-ignition method. *Ceramics International*. 2020;46:14481–14487. Available from: https://doi.org/10.1016/j.ceramint.2020.02.246.
27) Slatineanu T, Iordan A, Palamaru M, Caltun O, Gaftonand V, Leontie L. Synthesis and characterization of nanocrystalline Zn ferrites substituted with Ni. *Materials Research Bulletin*. 2011;46(9):1455–1460. Available from: https://doi.org/10.1016/j.materresbull.2011.05.002.
28) Xavier S, Thankachan S, Jacob B, Mohammed E. Effect of sintering temperature on the structure and magnetic properties of cobalt ferrite nanoparticles. *Nanosystems: Physics; Chemistry; Mathematics*. 2013;4(3):430–437.

29) Chen N, Gu M. Microstructure and microwave absorption properties of Y-subtituted Ni-Zn Ferrites. *Open Journal of Metal*. 2012;37:37–41. Available from: 10.4236/ojmetal.2012.22006.
30) Hezam FA, Khalifa NO, Nur O, Mustafa MA. Synthesis and magnetic properties of Ni0.5MgxZn0.5-xFe2O4 (0.0≤ x≤ 0.5) nanocrystalline spinel ferrites. *Materials Chemistry and Physics*. 2021;257. Available from: https://doi.org/10.1016/j.matchemphys.2020.123770.